Available online at www.sciencedirect.com
SCIENCE DIRECT®
Tectonophysics 380 (2004) 221–241
TECTONOPHYSICS
www.elsevier.com/locate/tecto

Active faults in the Zagros and central Iran

D.M. Bachmanov[a,*], V.G. Trifonov[a], Kh.T. Hessami[b], A.I. Kozhurin[a], T.P. Ivanova[c], E.A. Rogozhin[d], M.C. Hademi[e], F.H. Jamali[b]

[a] *Geological Institute, Russian Academy of Sciences, 7 Pyzhevsky Lane, Moscow 119017, Russia*
[b] *International Institute of Earthquake Engineering and Seismology, Tehran, Iran*
[c] *Institute of Dynamics of Geospheres, Russian Academy of Sciences, Moscow, Russia*
[d] *Institute of Physics of the Earth, Russian Academy of Sciences, Moscow, Russia*
[e] *Mahab Ghodss Co., Tehran, Iran*

Received 4 October 2001; accepted 28 September 2003

Abstract

Active tectonic movements in the northwestern Zagros include right lateral slip at the rate of about 10 mm/a along the Main Recent Fault, which inherits the position of the Main Thrust, now inactive, and active thrusting and accompanying folding distributed between several zones southwest of the Main Recent Fault. In the southeastern Zagros (the Fars Province), there are several right lateral faults that extend N–S obliquely to the overall trend of the Zagros fault-and-fold belt. These may be either branches of the Main Recent Fault, or faults accommodating relative broadening of the outer Zagros in its southeastern segment. The Main Thrust in the southeastern Zagros also remains inactive.

The Ipak, North Tehran, and Mosha fault zones and several minor structures in the eastern Alborz form the E–W-trending active fault system with combined reverse and left lateral slip. On the Ipak and Mosha zones, lateral movements with the late Quaternary mean rate exceeding 1 mm/a dominate over vertical fault movements. Together with right lateral faults stretching northeast of Zagros, the faults of the Alborz may accommodate east-directed motion of the Iranian microplate.

Keywords: Zagros; Active faults; Paleoearthquakes; Tehran region

1. Introduction

The basic contributions to studies of active faulting in Iran were made by Tchalenko (1975), Tchalenko and Ambraseys (1970), Tchalenko and Berberian (1975), Tchalenko et al. (1974), Berberian (1976, 1981), and others. The latest compilation of available data about active faulting is from Hessami and Jamali (1996).

In this paper, we address two questions. The first concerns active faulting in the region of the southeastern Zagros (the Fars Province), closer to where the single line of the Main Recent Fault of Zagros seems to terminate and where the Main Thrust Fault is inactive. The second question relates to kinematics of the E–W-trending faults in the Tehran region, south of the Alborz. These faults have always been interpreted as mainly thrusts and reverse faults with no significant strike–slip components of movement. At the same time, both the pattern of en echelon arrangement of the faults and left lateral slip on the west-

* Corresponding author. Fax.: +7-95-951-0443.
E-mail address: bachmanov@geo.tv-sign.ru (D.M. Bachmanov).

0040-1951/$ - see front matter © 2004 Elsevier B.V. All rights reserved.
doi:10.1016/j.tecto.2003.09.021

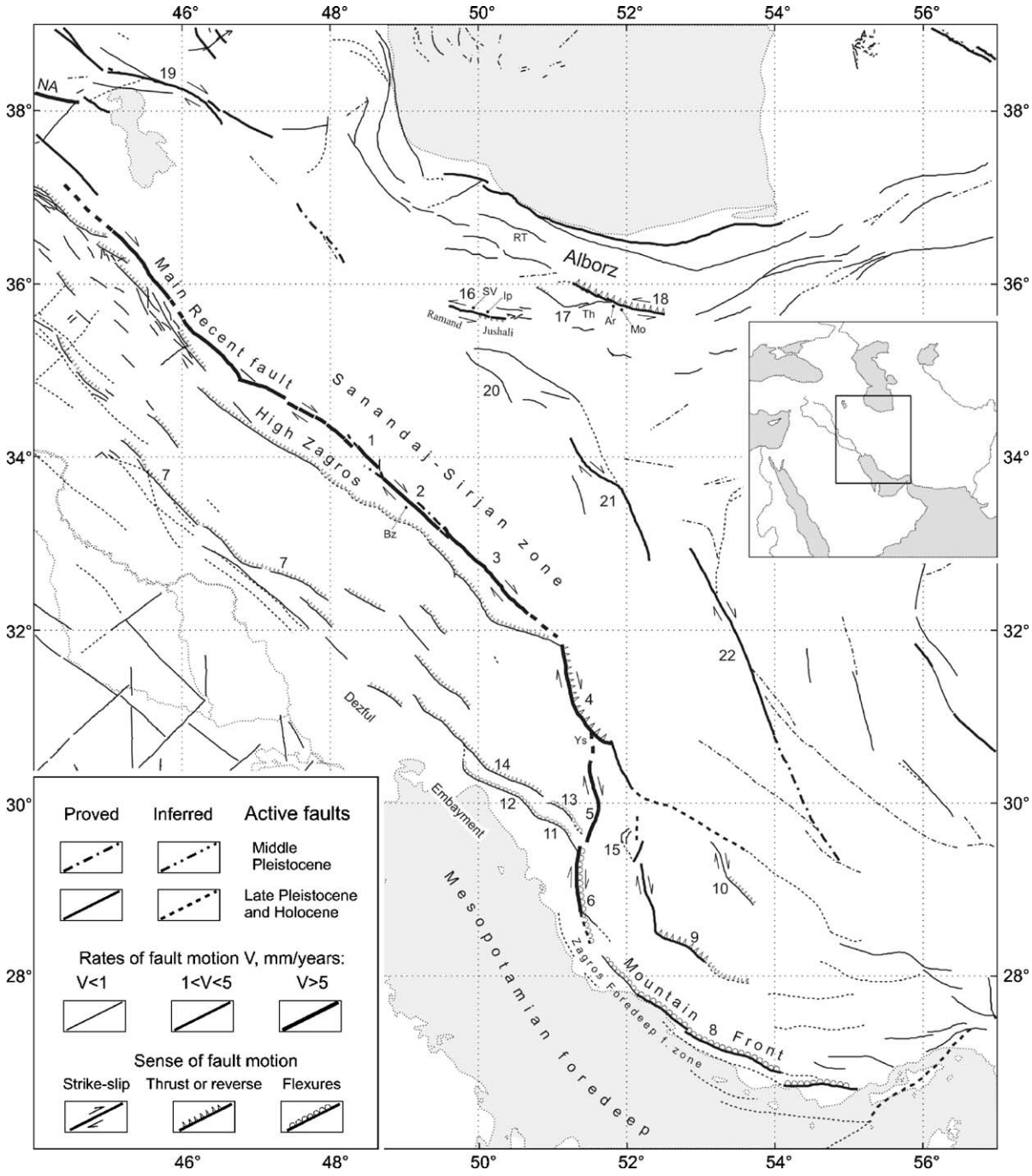

Fig. 1. Active faults in Zagros and central Iran. (1) Nahavand segment; (2) Dorud segment; (3) Ardal fault; (4) Dena fault; (5) Kazerun fault; (6) Borazjan fault zone; (7, 8) Frontal fault zone; (9) Kareh Bas fault zone; (10) Sarvestan fault; (11) Mazarei zone of flexures and faults; (12) Rag-e Safid fault; (13) Mishan flexure; (14) Aga–Jari thrust; (15) Dasht-e Arjan graben; (16) Ipak fault zone; (17) North Tehran fault zone; (18) Mosha fault zone; (19) North Tebriz fault; (20) Indes fault; (21) Kashan–Zephreh fault; (22) Deh Shir fault. Numerals preceded by ''T'' are locations of trenching (see text).

trending Rudbar – Tarom (RT in Fig. 1) fault during the 1990 earthquake of $M_s = 7.4$ (Berberian et al., 1992) suggest that strike-normal movements on the faults may combine with some sinistral slip. The faults run close to the densely populated area of Tehran, and this makes the problem of the sense and rates of movements along these faults important in terms of seismic hazard.

Below we describe the data obtained by field observations in the Tehran region and partly in the northwestern Zagros in 1996, and in 1998–1999 in the southeastern Zagros. The results were used for the ILP Project II-2 "World Map of Major Active Faults."

2. Active faults in the northwestern Zagros

Up to the middle Miocene, the Arabian plate interacted with the Iranian block along the Main Thrust of Zagros. Since the change in the direction of relative plate motion in the late Pliocene, the Arabian plate has been moving northward, obliquely to the Zagros chain. In the northwestern Zagros, the northwest-trending Main Recent Fault zone formed roughly in the same location where the Main Thrust was active earlier (Tchalenko and Braud, 1974; Berberian, 1976). According to these authors, the zone consists of several en echelon arranged segments with combined reverse and strike–slip movements. In its northwestern termination, the zone comes close to the North Anatolian fault zone (NA in Fig. 1), which moves predominantly right-laterally at the mean Quaternary rate exceeding 9 mm/a (Saroglu, 1988).

We visited the Nahavand and Dorud segments of the Main Recent Fault (1 and 2 in Fig. 1, respectively). Both segments form tectonic scarps between the High Zagros and the narrow intermountain basin that lies between the High Zagros and the highland of the Sanandaj–Sirjan tectonic zone further northwest. Each segment is represented by two (rarely three) nearly parallel branches, each of them producing topographic scarps. The northeastern branch is commonly younger. Along the Nahavand segment, this northeastern branch dipping 60° to the southwest performs both reverse and dextral movements. Thus, late Holocene ravines show 7–8 m of right lateral offsets, and bigger intersected valleys are bent laterally along the fault up to 100 m and more. On the southwestern branch of the segment, four large valleys are offset laterally by 1 ± 0.2 km.

The Dorud segment makes a right-hand step with respect to the Nahavand segment. Two branches, representing the Dorud segment, run along both sides of a river near the village of Bazazna (Bz in Figs. 1 and 2). Both branches, with the northeastern of them younger, perform reverse movements. Besides, the younger fault branch was found to offset 110–115 m right-laterally to a river valley. Where offset, the river valley is incised into the surface of an intermountain depression likely postglacial in age. This suggests that the observed dextral offset could have accumulated during last

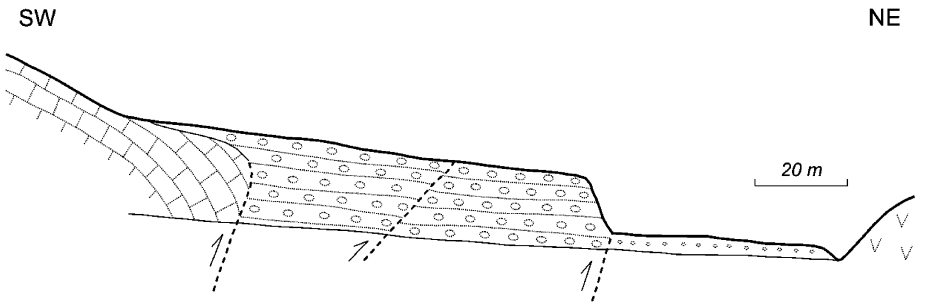

Fig. 2. The Main Recent Fault of Zagros in the northwestern side of the river near the village of Bazazna. The older western fault strand separates the Jurassic limestones and the second (late Pleistocene) river terrace, but does not affect the upper part of the terrace sediments. The younger eastern strand goes along the backstep of the first river terrace of the latest Pleistocene or probably early Holocene age.

10,000–12,000 years at the mean strike–slip rate of about 10 mm/a.

The Dorud segment is the one whose activity may have caused the 1909 Silakhor earthquake of $M_s = 7.4$ (Tchalenko and Braud, 1974; Tchalenko et al., 1974). According to our observations, 0.8–1 m of dextral and 0.25–0.3 m of vertical (southwest side up) offsets of small topographic features and stone-made fences between cultivated fields observed along the segment may be consequences of such earthquake.

A characteristic feature of the northwestern Zagros is that numerous young folds southwest of the Main Recent Fault strike parallel or very obliquely to the fault trend. The fold arrays are frequently bordered by either thrusts or flexures, probably above the tips of blind thrusts, with

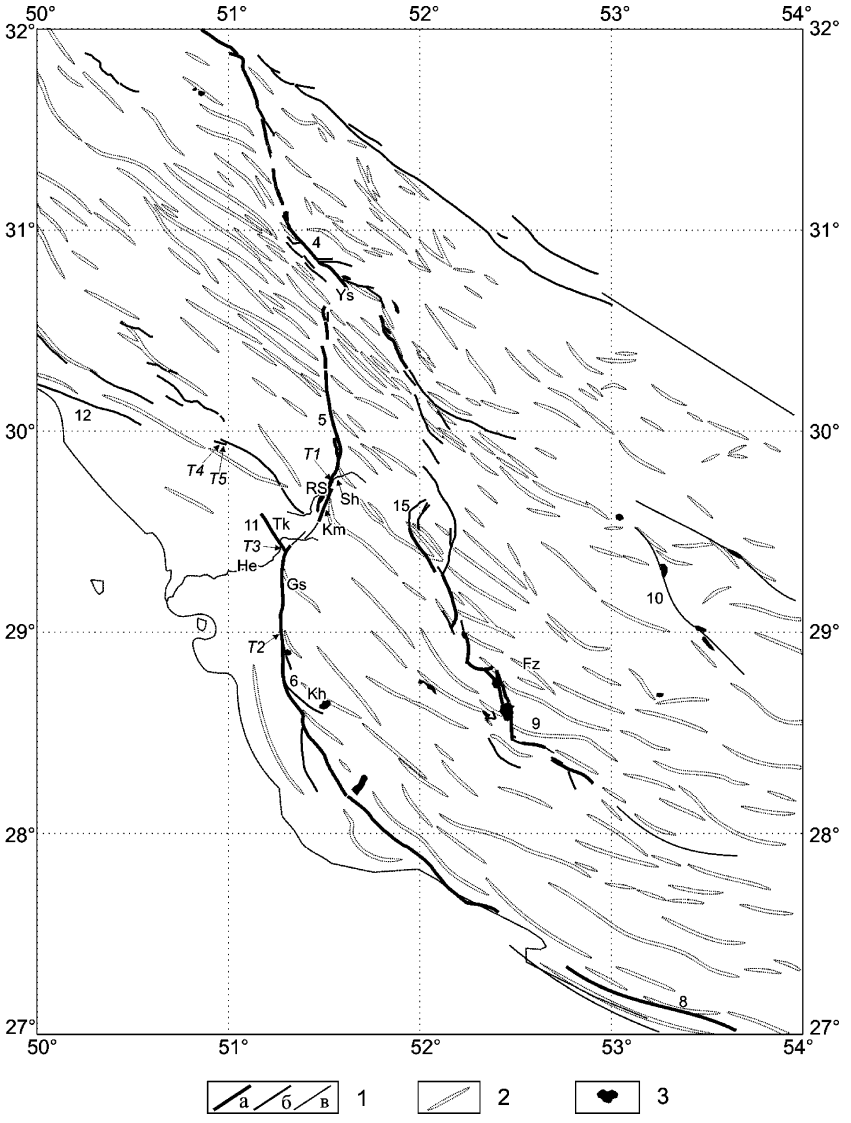

Fig. 3. Active faults in the southeastern Zagros (Fars Province). Axis of anticlines (undifferentiated by age) is from Tectonic Map of Southcentral Irân (1973) and Tectonic Map of Southwest Irân (1976).

manifestations of middle or late Quaternary activity. The largest of them are the High Zagros, Mountain Front, Dezful Embayment, and Zagros Foredeep fault zones (Berberian, 1976; Hessami and Jamali, 1996).

3. Active faults in the southeastern Zagros

3.1. Ardal and Dena faults

The 80-km-long Ardal fault (3 in Fig. 1) is the southeasternmost segment of the Main Recent Fault. Its southeastern termination is exactly where the Dena fault zone starts, extending south in a form of an arc curved southwest (4 in Figs. 1 and 3). The N–S-trending segment of the Dena fault splays in the south into several strands turning to the southeast. In the segment characterized by the change in the fault kinematics (about 25 km to the NW of the town of Yasuj; Ys in Figs. 1 and 3), three distinct strands of the Dena zone were identified. The northeastern of them makes a southeast-facing, 5-m-high scarp in the surface of the first (late Pleistocene) river terrace. One of large creek valleys shows also about 20 m of right lateral offset. The central strand, its plane dipping 75° northeast, separates Cretaceous limestones to the northeast from late Quaternary deposits to the southwest, which steeply dip away from the fault. Two branches, both with their southwestern sides uplifted, constitute the southwestern strand. Farther to the southeast, they merge with the central strand, making a single fault with the uplifted northeastern side.

No convincing evidences suggesting that the Main Reverse Fault within the southeastern Zagros is active have been found so far.

3.2. Kazerun fault

To the southeast of Yasuj, all the individual strands of the Dena fault demonstrate weaker late Quaternary activity, only vertical offsets, and no signs of strike–slip component. Near the town of Yasuj, another major fault, which is the 100-km-long Kazerun active fault, starts going southward (5 in Figs. 1 and 3). All along its length, individual fault planes are either vertical or steeply dip to the west. The northern part of the fault was found to perform only vertical movements, although striations on the fault planes, observed in places, may suggest some uncertainty in the amount of dextral components of movement. The E–W-trending, 100-m-long extensional fractures enlarged by karstic phenomena, rupturing the west fault side (Fig. 4), may be the features accommodating some part of the lateral slip along the fault.

Fig. 4. About E–W-trending karsted microgaben in the west side of the Kazerun fault zone south Yasuj. The trace of the Kazerun fault is shown by dashed line. Photo by V.G. Trifonov (view to the east).

Further to the south, recent activities of the fault and its dextral kinematics are more evident. Numerous right lateral offsets have been found at the foot of the mountainous west flank of the Rud-e Safid River valley (RS in Fig. 3), west and southwest of the ruins of the Sassanian capital of Bishapur (nowadays the Shahpur village; Sh in Fig. 3). Here, near the village of Ouladmizan, the anticline cored by the Miocene complexes is offset dextrally about

Fig. 5. Two strands of the Kazerun fault offsetting right-laterally the drainage system in the western side of the Rud-e Safid River. Photo by A.I. Kozhurin (view to the southeast).

750 – 800 m and vertically about 150 m, with the west side up. This yields a long-term ratio between two components amounting to 5. Offsets of the deepest gullies of the western slope of the Rud-e Safid River valley show 300 – 350 m of right lateral movements. In places, strike–slip movements along the fault caused capturing of one of the neighboring watercourses by the other. Further south, down to the village of Teng-e Tarkan, the fault provides a lot of good examples of displaced elements of drainage network (Fig. 5). Characteristic amplitudes of right lateral offsets measured there cluster around 3 – 5, 12 – 14, and 25 – 30 m. The faulted drainage within the downthrown east fault side entrenches a terrace-like surface. With the age of the surface remaining uncertain, we tentatively estimate the lateral displacements as late Quaternary. Vertical offsets are rarely observed, only in places amounting to 1–2 m.

The area is known for several recent earthquakes of magnitudes $M_s \geq 6$ (Moinfar et al., 1994), and the ruins of Bishapur still bear signs of previous seismic impacts of about the same magnitude, judging by historical records (Berberian, 1994).

We trenched the Kazerun fault where it crosses, in a form of a low scarp, a small triangle-shaped inlet of the depression surface. The Rud-e Safid River valley drains into the mountainous west fault side (at 29°45.952′ N and 51°31.541′ E; T1 in Fig. 3). The trench walls expose about the upper 3 m of mostly slope wash deposits accumulated at the depression margin. These are loam, loamy sand, and sand, partially calcareous, and intercalating with lenses and layers rich in debris of various grain sizes. Near the trench bottom, either bedrock or large boulders of Miocene gypsum outcropping west of the scarp may represent the base of slope wash material.

Basing on the content of coarser and finer materials, as well as on bedding pattern and partially absolute ages obtained, we identified all five sedimentary units (Fig. 6).

Unit 1, which is hard brownish loam nearly free of debris, was recognized only within the western sector of the trench. This unit is of Late Pleistocene, as the thermoluminescence (TL) age of 36,600 ± 6000 years of a sample collected in the upper part suggests. Well-layered unit 2 is represented by the same hard loamy sand and sand with extensive debris-containing lenses and layers. It is characterized by four TL ages, which are 8600 ± 970, 12,500 ± 420, 8750 ± 1080, and 11,350 ± 1200 years (see Fig. 6). Unit 3 is of the

same material but is looser, and with lenses of debris that are thinner and rarer. The upper part of the unit has the TL age of 9080 ± 870 years. Unit 4 was first identified to the east of the scarp as that of loose fine sediments with only the lens of debris and the TL age of its middle horizon being 7700 ± 700 years. West of the scarp, recognition of the same unit 4 is based on similar lithological composition and TL determination of 5200 ± 680 years. Finally, unit 5 is the soil profile annually subjected to plowing.

There is no clearly defined fault plane found except maybe for one or two fine steep fractures not extending above the top of unit 1. As the bearing of unit 2 evidences, deformation of the strata proceeded, first of all, through flexuring. Since no fault plane extends up the ground surface, we admit that the surface scarp has also undergone mostly flexuring, and that this flexuring is a specific manifestation of the fault movement in the upper relatively loose clastic sediments, close to the Earth's surface. Most likely, the fault plane projects upward to the foot of the flexure forelimb.

Paleoseismological interpretation of the deformations observed in the trench may be as follows.

We cannot say anything about the age of the fault seismogenetic movements that occurred prior to unit 2 accumulation, since the base of the unit in the downthrown eastern side is not exposed and, consequently, variation in its thickness, if any, remains unknown. Thus, our paleoseismological interpretation begins with unit 2 deformation. Important here is that the unit 2 layers show well-developed signs of sloughing and related distortion within the flexure forelimb (between fourth and seventh vertical marking lines). This suggests that unit 2 accumulated on the primarily more or less horizontal surface, and that flexuring occurred somewhat later. Evidently, prior to and during flexuring, unit 2 was not overlain by younger deposits; otherwise, its sediments could not move freely down the slope produced by flexuring.

Unit 3 is that found only to the east of the flexure. With its sediments leaning against the flexure forelimb and sealing slope deformations within unit 2, it can be readily interpreted as filling some surface depression above the lower limb of the flexure and therefore postdating this fault-related flexuring. The magnitude of vertical movement reached no less than 1.5 m, which is the approximate thickness of unit 4.

Available TL age determinations that could be used for constraining the age of that earthquake do not seem much certain. They feature roughly the same age of the upper parts of units 2 and 3, which are 8600 ± 970 and 9080 ± 870 years, respectively. With this, there seems to be no other possibility to admit a very high accumulation rate for unit 3 and age of the earthquake of around 9 ka.

The overlying unit 4 fills shallow surface depressions above both the upper and lower limbs of the flexure. Observable vertical separation of the unit is about 1.5 m, and this roughly equals that measured by the ground surface. It may be concluded therefore that the surface unit 4 accumulated on and the modern Earth's surface experienced the same obviously single deformation. There are no other sediments above unit 4 that would give the upper time limit for this last event. The lower limit is provided by the younger of the two TL ages obtained for unit 4, which is 5200 ± 680 years. Even younger are two radiocarbon ages of charcoal found beneath the soil horizon (see Fig. 6), which give 235 ± 80 and 690 ± 100 years. These may be, however, just remnants of man-made fire pots and lead thus to misinterpretation.

To summarize, we can say that the trench exhibits signs of at least two paleoearthquakes that occurred on the fault during last about 9 ka. During each of the earthquakes, vertical fault motion was around 1.5 m and caused the flexuring of the superficial strata. Based on the long-term ratio between right lateral and vertical components (see above), net slip during each seismogenetic fault movements can be estimated to have been about 7.5 m.

The above interpretation cannot be considered as definite in terms of recurrence intervals and amplitudes of individual fault displacements because, firstly, one more intermediate seismic event could have occurred, for example, during the accumulation of unit 2, although the observed portion of the unit strongly affected by seismic and postseismic movements does not give much keys for distinguishing it. Secondly, the foot of the monotonous slope where the fault runs has always been the area of unsteady and inconstant accumulation of clastic materials coming mostly through slope wash, and the units observed are most likely of local occurrence, both in space and in time.

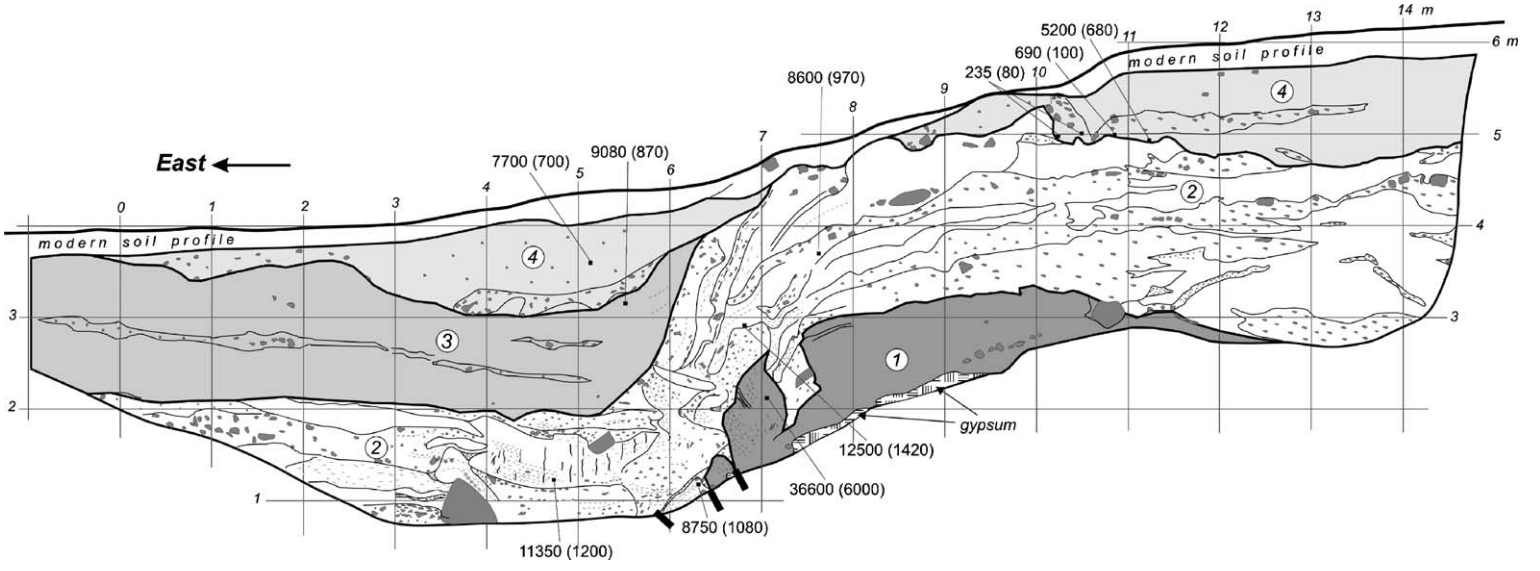

Fig. 6. South wall of the trench crossing the Kazerun fault (T1 in Fig. 3). Figures are the absolute ages (BP) obtained with the thermoluminiscenece method, except the youngest two values, which are the radiocarbon ages (standard deviations in brackets). Encircled numerals are the horizons unidentified (see text).

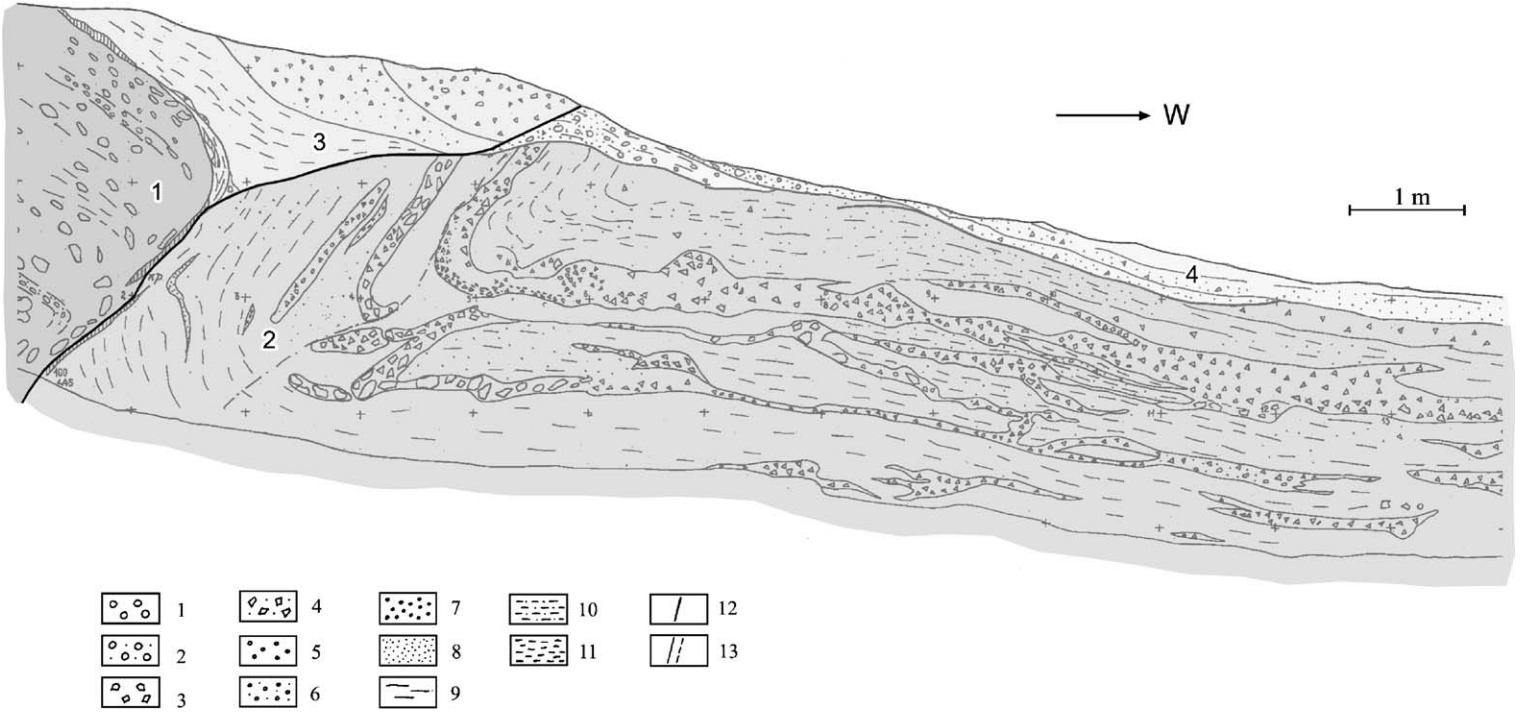

Fig. 7. One of the reverse faults of the Borazjan zone in the upper part of upper Pleistocene and Holocene alluvial–proluvial deposits southeast of Ahram (28°52.31′ N and 51°17.71′ E; T2 in Fig. 3). Numerals stand for lithologically different sedimentary units, which are alluvial well-rounded gravel and pebble with coarse sandy matrix (1), loam with intercalations of lenses and layers of limestone and marl debris (2), slope wash and proluvial loam with clasts of limestone, their content increasing upward (3), and Holocene loose alluvial sand with numerous small gravels of limestone.

The southern segment of the Kazerun zone demonstrates evidences of oblique (combined right lateral and vertical) Quaternary motion, but some manifestations of the Late Quaternary activity were found only near the village of Kamaraj (Km in Figs. 1 and 3). Further to the south, the Kazerun fault as an active one seems to disappear.

3.3. Borazjan fault zone

Hessami and Jamaly (1996) consider the Borazjan fault zone, around 80 km long (6 in Fig. 3), and the Kazerun fault as two segments of a single structure. Although signs of the recent activity of the Borazjan zone are numerous, there are no direct evidences of strike–slip offsets of geomorphic elements. The only possible way to estimate net lateral displacement along the zone is to correlate it with about 10 km of lateral bending of the Gisakan – Takab anticline (Gs and Tk in Fig. 3) between terminations of the Kazerun and Borazjan zones. Upper Pliocene to lower Pleistocene alluvial conglomerate and sandstone of the western side of the asymmetric Gisakan – Takab anticline dip steeply and, in places, vertically. There is a weak angular unconformity of 10–15° between alluvium and upper Miocene complexes below. This suggests that folding and lateral drag began before alluvial accumulation and that most severe deformations took place during and after. As lower alluvial layers were formed during the Matuyama magnetic epoch before the Olduvai episode (Bachmanov, 2001), we interpret the 10-km dextral bending of the anticline as late Pliocene – Quaternary in age (last 2 – 2.5 million years) and hence estimate the long-term lateral slip rate to be 4 – 5 mm/a.

Supposed dextral kinematics of the Borazjan zone could also account for clockwise rotation of the

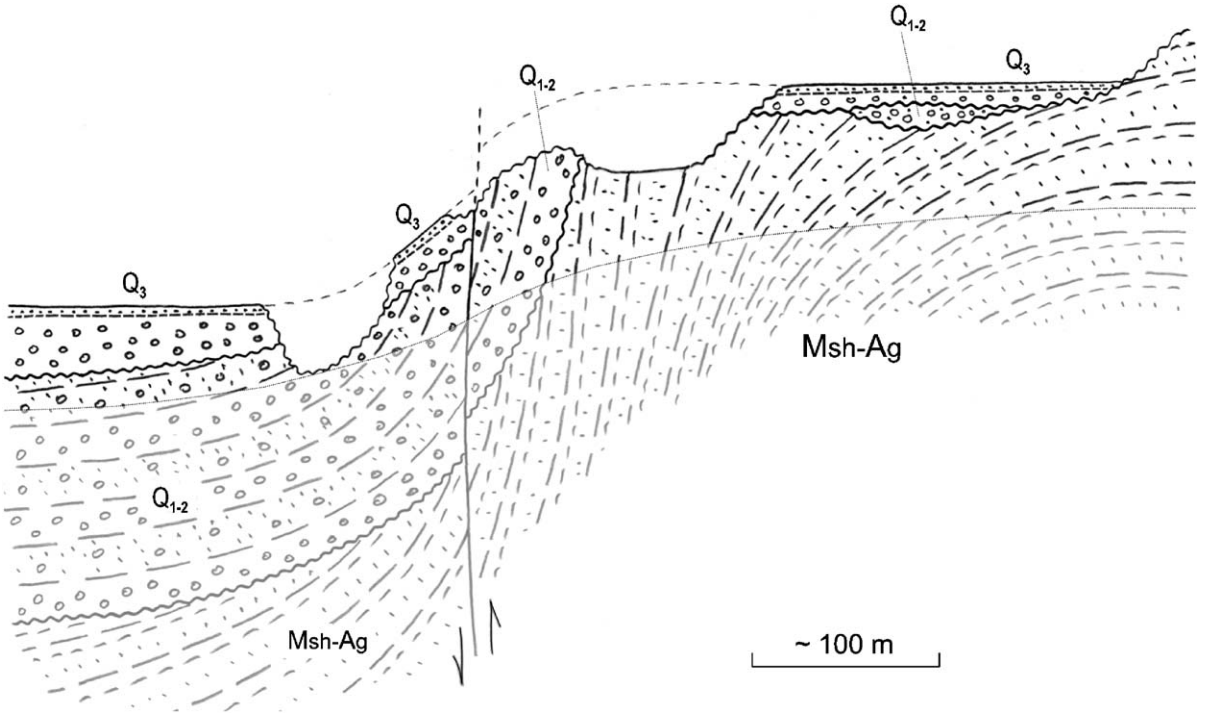

Fig. 8. Principal cross-section of the Mazarei fault flexure zone in the north side of the Helleh River. Msh–Ag is Middle Miocene to lower Pliocene Mishan and Agha Jari Formations undifferentiated. Q_{1-2} and Q_3 are upper Pliocene and lower–middle Pleistocene and upper Pleistocene alluvial deposits. The unconformities are observed between Msh – Ag and Q_{1-2}, and between Q_{1-2} and Q_3. The Q_{1-2} deposits are thicker in the western downstream side of the fault flexure scarp.

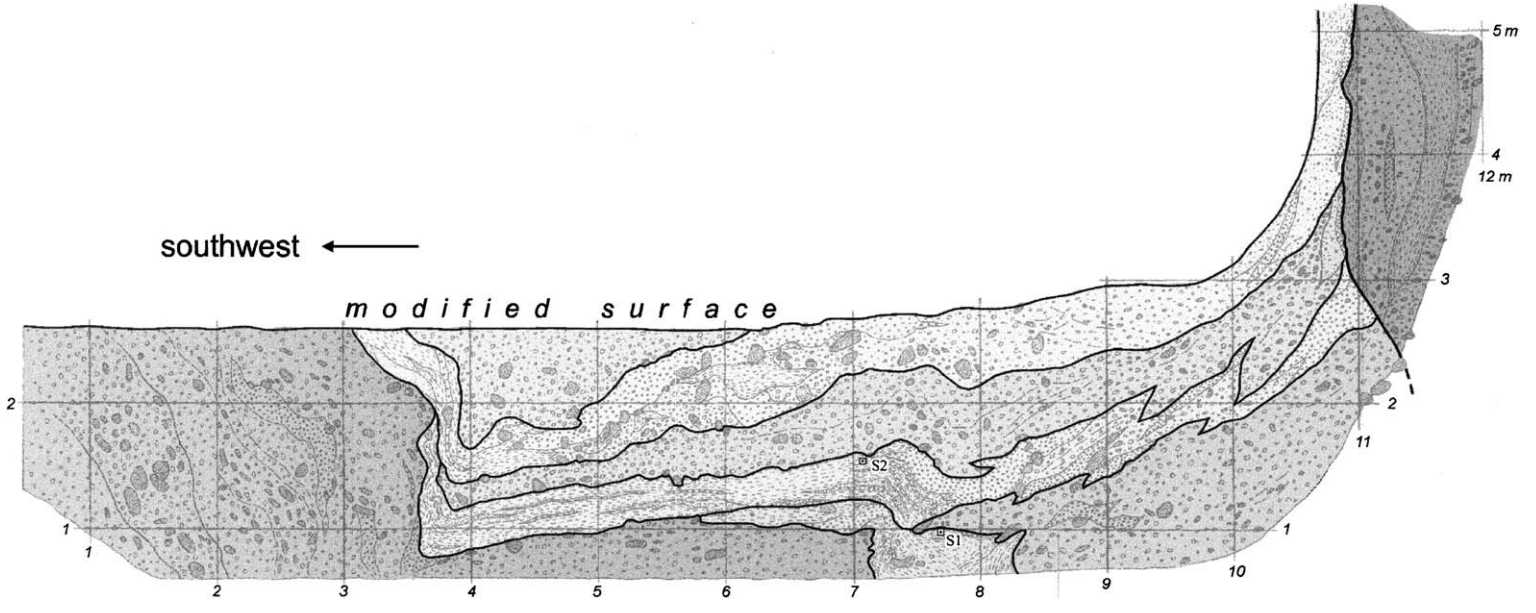

Fig. 9. Northern wall of the trench crossing the Mazarei fault flexure zone south of the Helleh River (T3 on Fig. 3). S1 and S2 are the sampling points (see text).

northern parts of some of the anticlines of Zagros where they come close to the zone.

3.4. Mountain Front fault system (frontal zone)

Located as a prolongation of the Kazerun fault (5 in Fig. 3), the Borazjan zone is at the same time a segment of the Mountain Front Fault System (Frontal zone) between its NW-trending parts northwest and southeast of the Kazerun fault (7 and 8 in Fig 1, respectively). The Borazjan zone is expressed first of all as a high surface scarp between the Zagros elevation and piedmont plain. From a structural point of view, this is a large flexure, or rather a set of en echelon organized minor flexures that have likely formed above the tip of a major blind fault zone. Rare low-amplitude reverse faults of the zone reaching the land's surface were found to affect the middle Pleistocene and Holocene sediments at the foot of the scarp (T2 in Figs. 3 and 7).

The southern segment of the Mountain Front Fault System, the Borazjan zone, merging within the south, includes two parallel strands of flexures and thrust faults. Together with the Borazjan zone, they form a single arched structure similar to that of the Dena zone far to the north.

3.5. Kareh Bas fault zone and Sarvestan fault

The Kareh Bas fault zone (9 in Figs. 1 and 3) starts close to the southeast end of the Dena fault, then goes first south obliquely to folds of Zagros and then to the southeast parallel to the folds, commonly along their southwestern steeper limbs. Southwest of Firuzabad (Fz in Fig. 3), two individual faults of the zone together display 6 km right-laterally a large anticline, one of them going there right across a large salt dome that emerges through the anticline crest. South of the salt dome, the fault planes dip steeply to the east. Quaternary conglomerates of the western fault side dip away from the fault and are inclined $70-90^\circ$ or even overturned closer to the fault. The fault displaces right-laterally watercourses and other young landforms, the offset values ranging from $2.5-3$ to $10-20$ m and up to 45 m. Three larger valleys are offset laterally by $90-100$ m.

Further to the south, the strike of the Kareh Bas zone gradually changes to southeast and becomes a flexure accompanied by thrusting. It serves as the boundary between the High Zagros and the Lower Zagros.

The Sarvestan fault (10 in Figs. 1 and 3) presents a relatively small faulting feature of the Fars Province,

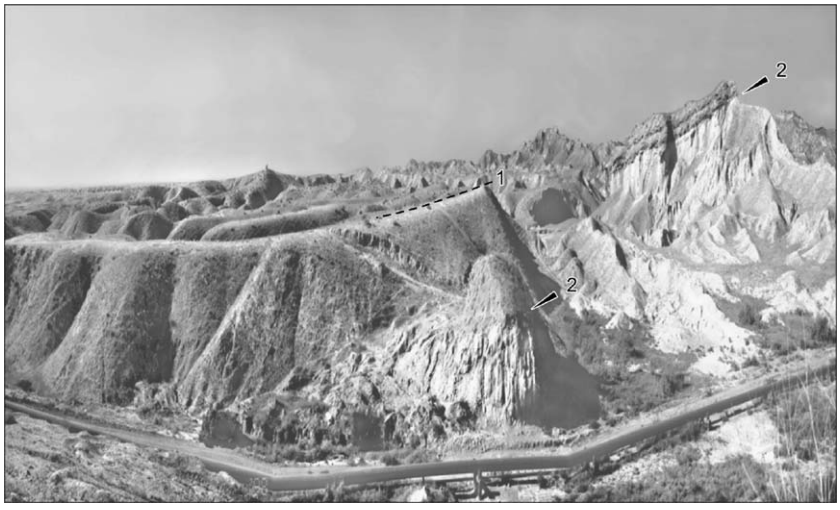

Fig. 10. The Rag-e Safid fault flexure zone near the Ganaveh – Behbahan road. The arrows numbered 2 point at the base of the Middle–Upper Pleistocene sedimentary cover of the flat piedmont plain. The plain surface (1) is getting noticeably steeper (up to 6°) northeastward, closer to the fault flexure zone. The lower Quaternary deposits lie much steeper than the younger sediments do, and they are overturned near the fault-flexure that dips there about 60° northeast. The Middle–Upper Miocene Mishan formation of the northeastern side is overthrusted onto the younger Agha Jari formation. Photo by A.I. Kozhurin.

stretching northeast and parallel to the Kareh Bas zone.

3.6. Mazarei zone and Rag-e Safid fault

Northwest of the Kazerun – Borazjan zone, the Mountain Front Fault System is represented by two strands, the southwestern of them including the Mazarei flexure and the Rag-e Safid fault (11 and 12, respectively, in Figs. 1 and 3). The Mazarei zone of flexuring and, to a less degree, faulting goes along the southwestern flank of the asymmetrical Takab anticline (Tk in Fig. 3). The upper Pliocene, and lower and middle Pleistocene 60-m-thick consolidated alluvial deposits of the anticline southwestern limb steeply dip (in places, vertically) to the west (Fig. 8). Fragments of the same alluvial sediments, up to 5 m thick, covering the anticline closer to its core lie horizontally. On the trace of the Mazarei fault zone, they are overlain with angular unconformity by the upper Pleistocene loose alluvial deposits of the Helleh River terrace (He in Fig. 3), which show up to 20° dip also to the southwest. West of the Mazarei zone, dip angles of both consolidated and loose sediments as well as the unconformity surface between them are getting progressively shallower with the distance from the zone.

The scarp of the Mazarei zone was trenched several hundred meters south of the Helleh River (at 29°28.26′ N and 51°16.74′ E; T3 in Fig. 3). The trench is located on an artificially leveled surface cut down to about 5 m into the terrace deposits of the Helleh river.

Sediments exposed by the trench are layers and lenses of alluvial well-rounded gravel and pebbles and sand of varying grain sizes (Fig. 9) probably mixing with some slope wash deposits. Angular or poorly rounded pieces of rocks are rare, emphasizing the insignificant contribution of colluvial material supply. Clear stratification of strata is emphasized by intercalation of coarser and finer clastic sediments. All the layers are folded into an asymmetrical syncline, with its western limb being vertical.

The absence of any convincing evidences that folding proceeded in a constant manner provides the possibility to interpret it as resulting from shortening and to correlate the latter with a sudden westward advancement of the Mazarei flexure forelimb. A minimal amount of lateral shortening may be evaluated by the observed length of the syncline vertical limb, which is at least 1.5–2 m. Available TL age determinations (7500 ± 650 and 6900 ± 1250 years BP, samples S1 and S2, respectively, in Fig. 9) provide the lower time limits of the tectonic movement and the corresponding seismic event. Most probably, it occurred well after the younger of them.

The northern bank of the Helleh River still exhibits remnants of ancient irrigation channels, probably of the Sassanian epoch. In two localities, the channels are faulted with vertical displacement of 0.5–0.6 m, evidencing fault-related seismic motions of the historical period.

As in the Mazarei zone, a flexure and several steep reverse faults of the Rag-e Safid zone disturb the southwestern limb of an anticline (Fig. 10).

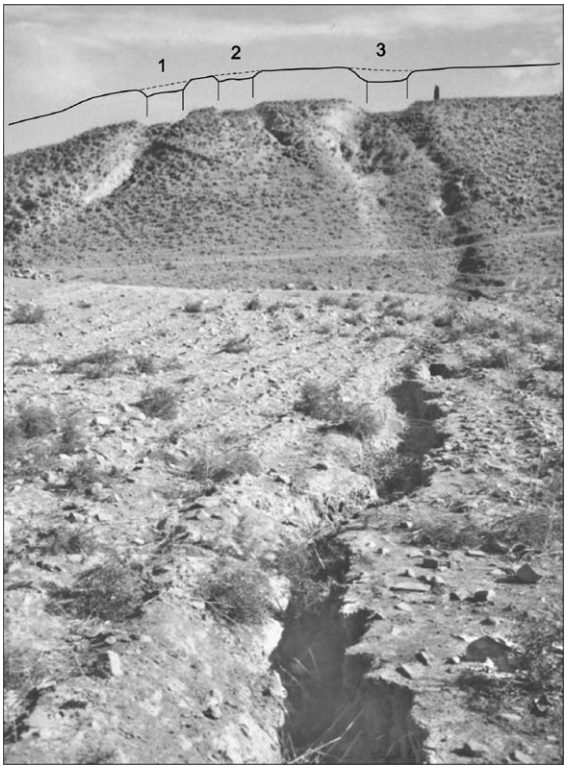

Fig. 11. Three shallow grabens within the Mishan 1972 earthquake fault zone. Photo by A.I. Kozhurin.

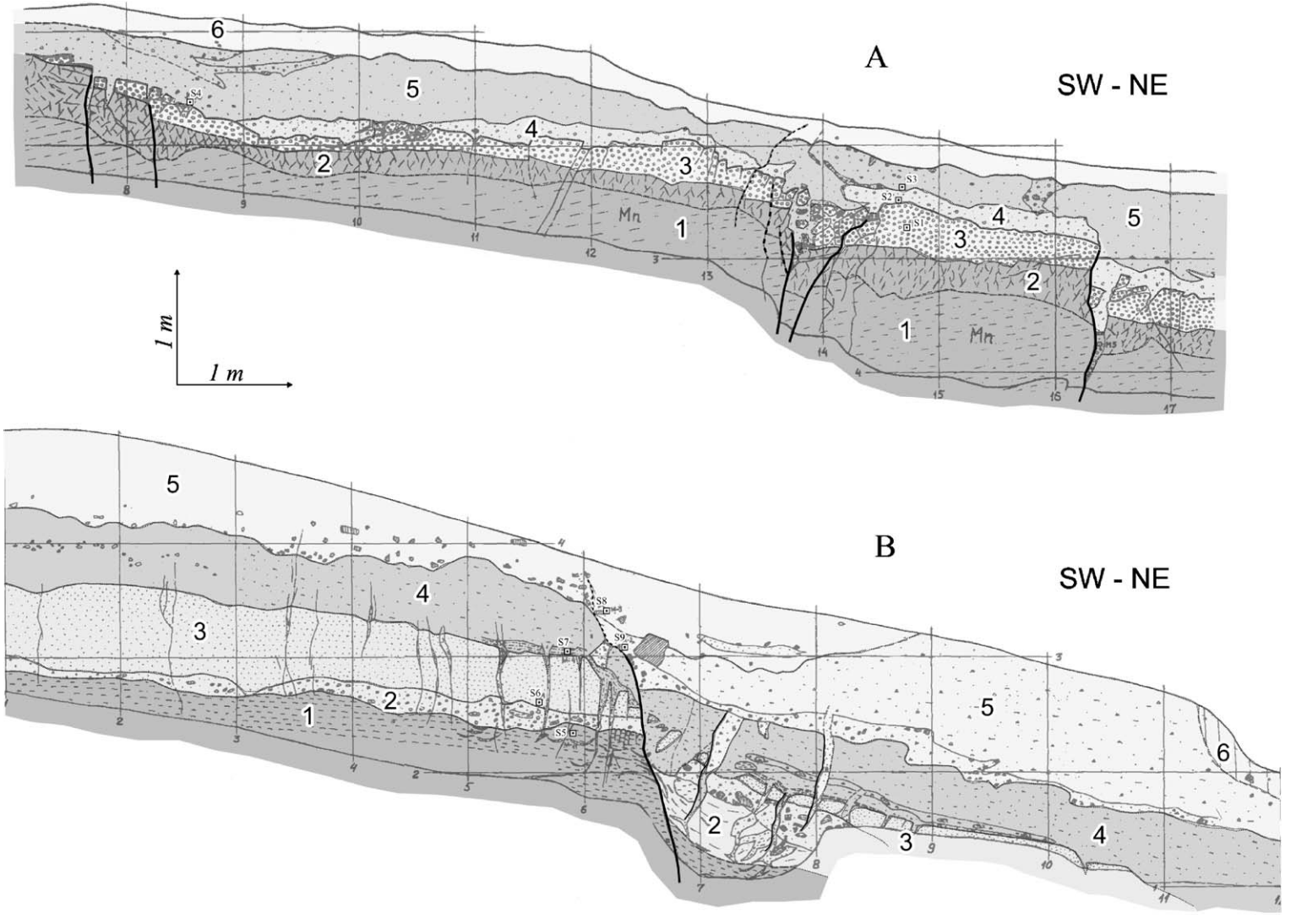

Fig. 12. Logs of two trenches across the Mishan 1972 earthquake fault zone (T2 and T3 on Fig. 3). Numerals are identified stratigraphic units. Vertical and horizontal lines follow through a meter. Manifestations of three seismic events are identified in the trenches. The latest event probably corresponds to the 1972 earthquake. A and B are the western trench and the eastern, trench, respectively (see text).

3.7. Mishan flexure and Aga–Jari thrust

The northeastern strand of the Mountain Front Fault System is represented by the Mishan flexure and the Aga–Jari thrust (13 and 14, respectively, in Figs. 1 and 3). The latter runs parallel to the Rag-e Safid fault along the steeper southwestern limb of an asymmetrical anticline and dips $20-30^\circ$ to the northeast (Berberian, 1976).

The 10-km-long zone of shallow grabens and normal faults disturbs the Earth's surface in front of the Mishan flexure (Fig. 11). The zone is known as the 1972 Mishan $M=5.5$ earthquake epicentral area and is characterized by creep and frequent weak to moderate earthquakes.

We made two trenches to cross two of the surface scarps of the zone (Fig. 12; T4 and T5 in Fig. 3).

The western trench (29°59.21′ N, 50°58.12′ E) is located on the surface where it is gently sloping towards the Mishan flexure, which is about 1 km north. Structurally, the slope is the northern limb of a low-active anticline paralleling the Mishan flexure.

Strata exposed in the walls of the trench are subdivided into six units. These are: (1) bedrock (the Miocene Mishan Formation); (2) fractured bedrock; (3) layer of weathered bedrock with the TL age of its lowest part being $21{,}700\pm2400$ years (S1 in Fig. 12); (4) coarse part of the Holocene slope wash deposits, with the TL age of its lowest horizon being $14{,}000\pm1500$ years (S2 in Fig. 12); (5) finer part of slope wash deposits TL-dated as 7000 ± 900 and 7100 ± 1100 years (samples S3 and S4, respectively, in Fig. 12); and (6) recent soil. Three faults are observed cutting through different units, of which only units 4 and 5 are sedimentary.

3.7.1. Central fault

This one displays both the Earth's surface and bedrock with the same vertical amplitude of about 0.5 m. This suggests that all the units experienced equal numbers of seismogenic fault movements. Because no variations in thickness of the units across the fault are observed, and there are no deposits overlying the soil profile within the downthrown fault side, the event horizon for this latest event is the Earth's surface. Most likely, that was the event of 1972.

3.7.2. Southern fault

The fault does not produce a surface scarp and does not display the top of unit 5. Unit 5, at the same time, is thicker in the downthrown side of the fault, at the foot of the fault-related slope, about 0.5 m high, made by the surface of weathered Miocene bedrock. All this suggests that the event horizon for the event may lie between the base of unit 5 and weathered bedrock, and the age of the event may be a little older than about 7000 years (constraining ages are those of the samples S4 and S3). Less possible but probable seems the variant that the event took place prior to accumulation of unit 4 (i.e., some time before 14,000 years back—the age of the sample S2) because unit 4 is observed only within the downthrown fault side.

3.7.3. Northern fault

This one is very similar to the southern fault. Again, it offsets neither the Earth's surface nor the upper surface of unit 5, which, unlike the lower stratigraphic boundaries, shows the same increase in thickness within the downthrown fault side. Undoubtedly, the event took place after accumulation of unit 4 but before accumulation of the lowermost horizon of unit 5. The vertical separation during the earthquake was again about 0.5 m.

To summarize, the paleoseismological interpretation of the western trench is as follows.

The last event occurred after the formation of the modern soil profile and the Earth's surface. Most likely, that was the event of 1972. The penultimate event took place on the northern fault about 7000 years back. The age of the earthquake that was caused by vertical movement along the southern fault remains uncertain. It was either the same penultimate or another one about 7000 years older. Interpreting two earthquakes implies, therefore, 0.5 m of the last vertical fault separation, about 1 m for the penultimate vertical fault movement, and about 7000 years as the recurrence interval, while interpreting three earthquakes yields 0.5 m per event and the same roughly 7000-year long interval between them.

The eastern trench (29°59.154′ N, 50°58.361′ E), some 200 m east of the first one, exposes the strata beneath a fault-related surface scarp within a shallow river valley. The river used to be heading southwest, and has been abandoned since the Earth's surface in

front of the Mishan flexure gained northeast-directed tilt due to development of the flexure-parallel low anticline. At present, water is flowing southeastward along the Mishan flexure.

We identified five units in the walls of the eastern trench. Unit 1 is marl and clayey marl of the Miocene Mishan formation, with its uppermost decomposed and weathered horizon dated by TL as 22,000 ± 3450 years (S5 in Fig. 12). The unit 2 above is a layer of fine and moderate-sized marl debris, sometimes poorly rounded, up to 0.4 m thick. Unit 3, 0.5–0.7 m in thickness, is represented mostly by yellowish gray fine to moderate—in places clayey—sand. The TL age of sample S6 taken from the unit 3 lowermost horizon is 6900 ± 610 years. Unit 4 is brownish loamy sand, 0.4–0.5 m thick, with TL age of its lowermost part being 3700 ± 350 years (S7 in Fig. 12). Unit 5 is represented by darker brownish looser loamy sand and sandy loam with fine debris and lenses of coarser debris. The fault is represented by a single plane steeply dipping north. The thickness of unit 5 varies along the wall from about 0.6 m in the south through 0.3–0.4 m in the middle of the trench, above the fault, to around 1 m east of the fault. There is also a surface scarp above the fault. Based on the fact of evidently too low thickness of unit 5 immediately south of the fault (0.3–0.4 m), we interpret that the observed scarp slope is modified and the corresponding part of the unit 5 material has been removed by some surficial process.

In either fault sides, all the units show a gentle northern dip, which is the dip of the northern limb of the anticline that parallels the major Mishan flexure around 1 km to the north. Implying that true thickness of unit 5 in the south fault side is that observed in the southernmost part of the trench, far from the scarp, and that the Earth's surface in the southern fault side was primarily also parallel to stratification, we extrapolate the Earth's surface as shown in Fig. 12 and estimate the magnitude of its vertical separation as not exceeding half a meter.

All the unit boundaries up to the base of unit 5 are offset vertically by the same amplitude of roughly 1 m. Unlike the lower units, which maintain their thickness as approximately the same in either fault sides, unit 5 shows increase in its thickness from about 0.5–0.6 m to roughly about 1 m. Vertical fault separation of the Earth's surface is about 0.5 m, and there are no sediments covering the surface. We conclude from these facts that the modern Earth's surface is the event horizon for the last fault movement, and that the event horizon for the penultimate event lies between units 4 and 5. During each of the seismic events, vertical offset on the fault was about 0.5 m.

The last event was most probably that of 1972. The age of the penultimate earthquake cannot be defined with certainty based on the available TL ages. The matter is that TL ages obtained for unit 5 from immediately north of the fault (14,300 ± 2020 and 6100 ± 700 years, samples S8 and S9, respectively, in Fig. 12) turn out to be too old if compared with TL age of 3700 ± 700 years obtained for the base of unit 4 (sample S6) south of the fault. Moreover, these two ages alone show a reverse stratification, with older materials higher in the section. On the contrary, all the TL ages from the southern fault side follow normal time ordering. Without the ages from the eastern fault sides, it can be interpreted that the penultimate event took place after about 4000 years BP, and that the interval between the two earthquake was shorter than 4000 years.

It is worth noting that the faults exposed in the trenches described above are not the only ones in the epicentral area of the 1972 Mishan earthquake, and our estimations of the recurrence interval (about 7000 and less than 4000 years) between strong earthquakes in the area may not be true. There seem to be more reliable measurements of individual (or characteristic) vertical offsets; these range from 0.5 to 1 m. Based on the empirical relation of Wells and Coppersmith (1994), both the length of the zone of grabens and normal faults, which is about 10 km, and the magnitude of an individual seismogenic offset yield roughly 6.5 as the magnitude of paleoearthquakes.

3.8. Dasht-e Arjan graben

The Dasht-e Arjan graben (15 in Figs. 1 and 3) is expressed in topography as an N–S-elongated low with fault scarps along both sides. In the southern part of the graben, the western boundary fault strikes N10°E and steeply dips to the east. The fault demonstrates a combination of normal and right lateral movements, as emphasised by a 35-m dextral offset of one of the intersecting creeks. Northerly,

Fig. 13. Exposed part of the fault plane of the northwestern border of the Dasht-e Arjan graben. The lowest lighter part of the plane marks the last offset. Photo by A.I. Kozhurin.

both bounding faults of the graben gain the N25°E trend and, judging by striation on the fault planes, are mostly normal. Uplifted sides of the graben are composed of Lower Miocene limestone. Cumulative vertical offset on the northwestern boundary fault scarp is about 150 m. Darker upper and lighter lower parts of the slope, which is the exposed fault plane, are well discernible (Fig. 13). The lighter part of the fault plane surface, smooth and clean, is 0–22 cm wide (up to 60 cm locally). The darker part is slightly eroded and covered with lichens in colonies of up to 5 cm in diameter. Similar variations in texture of a single fault plane were first observed by Wallace (1977) in Nevada and interpreted as evidencing coseismic displacements. The age of the earthquake can be estimated by assuming that the fall of boulders piling now at the base of the scarp was triggered by the same seismic event. The boulders cover the surface of Quaternary sediments that dip away from the scarp. The surface is cut by a narrow gorge. The uppermost part of its alluvium contains ceramics of the medieval type. The thermoluminescence analysis of the ceramics yielded the age of about 700 years BP (determination of the Museum of Ancient History, Tehran). According to these data, we tentatively estimate the age of the earthquake by several hundred years. Probably, it occurred not earlier than 700 years BP.

The same variations in shade and texture were observed on the plane of the southeastern boundary fault. In all, there are three different parts of that fault plane, the lower two of them being as wide as about 10 and 20 cm. The wider intermediate part can be interpreted as marking a previous strong earthquake. As the last earthquake in the Kareh Bas fault zone occurred in 1999 ($M_s = 6.2$) the recurrence interval of earthquakes of $M_s \geq 5.5$ along this structure may be evaluated to be several hundreds of years.

So, the southeastern Zagros demonstrates a combination of the N – S-trending dextral faults and the NW-trending thrusts and reverse faults, the latter often accompanied by flexuring in upper layers of the sedimentary cover. The small graben-type structures generating more frequent but weaker earthquakes may mark the areas subjected to local tectonic extension.

4. The west-trending fault system to the south of the Alborz

South of the Alborz, active faults are represented by the major Ipak, North Tehran, and Mosha faults, and a number of minor faults between. While a common interpretation suggests that all the faults in the area move predominantly as thrusts and reverse faults, en echelon arrangement of individual faults indicates the presence of some lateral component of motion as well.

4.1. Ipak fault zone

The 100-km-long Ipak zone (16 in Fig. 1) is a combination of the W- and WNW-trending segments striking along the Ramand Mountains and the Jushali and Jaru Ridges. The main segments show stepwise

arrangement. The western part of the zone was ruptured during the 1962 Buyin Zara earthquake (M_s = 7.25) associated with 1 m of reverse component combined with up to 10 cm of left lateral component (Ambraseys, 1963). The Late Quaternary reverse offsets are common for all the segments. Along the western side that dips 60 – 80° south, the southern side is uplifted. For example, 1 km west of the village Sura Vagin (SV in Fig. 1), the lower and middle Pleistocene alluvial deposits show a vertical offset of 2–3 m. The central segment running across the village of Ipak dips 60° to the north and has its northern side uplifted. The small graben within the downthrown fault side is filled with Pleistocene and Holocene gravels.

Oblique striations on the fault plane observed west of the village of Sura Vagin give a ratio between sinistral and reverse components of 2 – 3 to 1. Near the village of Ipak (Ip in Fig. 1), the stream incised into the northern side of the fault produces an asymmetric alluvial fan within the southern fault side. Location of the oldest fan generation suggests 85–90 m of left lateral separation along the fault (Fig. 14a), while the younger fan lies just in front of the river outlet. The same asymmetry is characteristic of other fans near the fault. On the southern slope of the Jushali Ridge, the late Pleistocene terraces of two large river valleys are offset 25 – 30 m left-laterally along the W-trending strand of the fault zone (Fig. 14b). In summary, the Ipak fault zone shows evidences of both reverse and sinistral slip, with the strike–slip probably dominating.

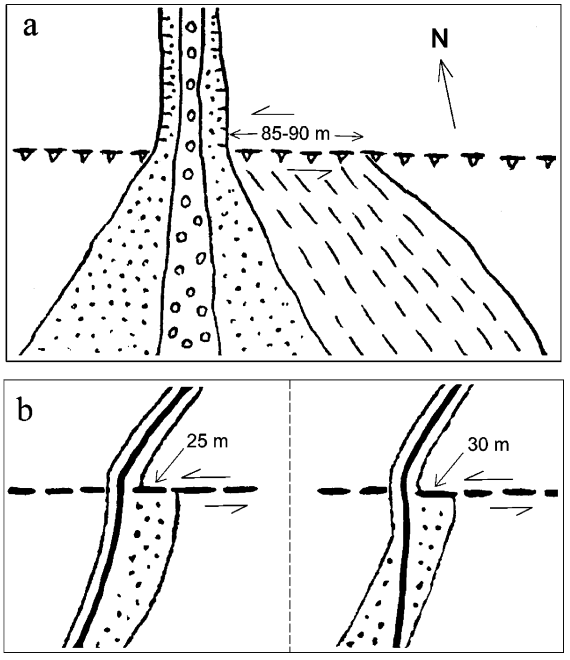

Fig. 14. Evidences of the left lateral slip along the Ipak fault zone. (a) Displacement of the alluvial fan relative to the upstream part of the valley near the village of Ipak. (b) Two creek valleys offset right-laterally at the foot of the southern slope of the Jushali Ridge.

4.2. North Tehran fault zone

The North Tehran fault zone (17 in Fig. 1) was described in details as one with mostly thrust movements (Tchalenko, 1975; Berberian, 1976). The 100-km-long zone is arched to the south and roughly follows the drainage divided between the Alborz elevation and the Pleistocene alluvial plain. There are numerous convincing evidences of thrust movements on both the western (NW-trending) and eastern (ENE-trending) parts of the zone. One of the youngest fault segments in its eastern part may also have some sinistral components of movements. So, south of the Shahid University in the northern margin of the City of Tehran (Th in Fig. 1), the eastern slope of the Darakeh River valley north of the fault seems to be located about 150 m left relative to the same slope south of the fault. We should admit, however, that this conclusion is largely tentative as the city constructions strongly obscure the probable lateral offset.

4.3. Mosha fault zone

In the east, the North Tehran fault joins the WNW-trending Mosha fault zone (18 in Fig. 1). The fault zone, more than 175 km long, consists of several segments arranged in a stepwise manner. All along the zone, the northern fault sides are uplifted. The fault planes observed show northeastern dips of about 60°. Gentler dip of 35–55° was observed in the fault segment 1.5 – 2.5 km east of the village of Mosha (Mo in Fig. 1), where Upper Precambrian dolomites are thrusted onto late Upper Pleistocene moraine and fluvial–glacial deposits gently (5°) dip southward parallel to the intermountain basin surface (Fig. 15b). At the same time,

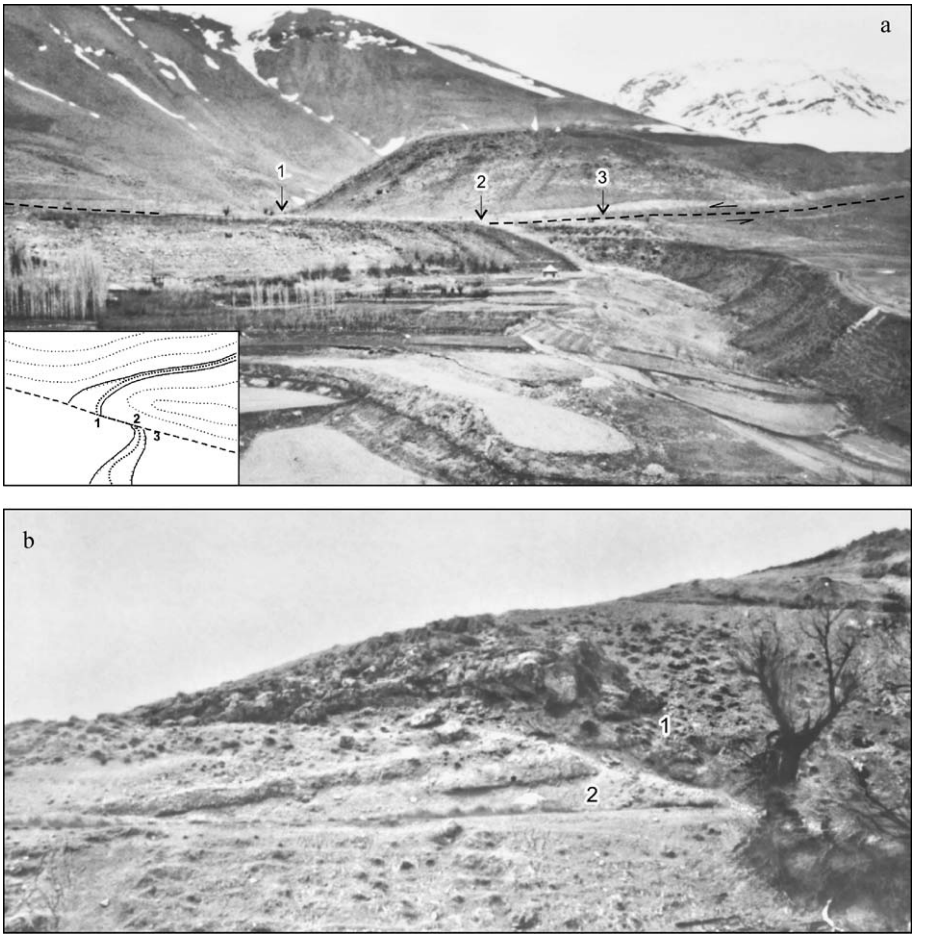

Fig. 15. Evidences of active faulting along the Mosha fault zone. (a) The valley is incised into the Upper Pleistocene moraine and fluvial–glacial deposits in the southwestern side of the fault are offset 25 m left-laterally. Dashed line follows the base of the fault scarp. Inset is a plan view of the offset site. On photo and inset: 1–2, fault offset of the stream; 1–3, the total offset including drag component. (b) Thrusting of the Upper Precambrian dolomites (1) onto the Upper Pleistocene moraine and fluvial–glacial deposits (2) 2.5 km east of the village of Mosha. The fault plane dips 35 – 55° northeast.

shallow Holocene ravines near the village of Javard are systematically offset or bent several meters left-laterally along the fault. Larger sinistral offset of about 25 m was measured by the valley 0.5 km to the east of the Mosha village (Fig. 15a). As the valley is entrenched into the upper Pleistocene glacial and fluvial–glacial deposits, the offset must have accumulated during the Holocene time with the mean rate of lateral slip of 2–2.5 mm/a. The 20-m sinistral offset of a similar valley was observed also 1.5 km east of Mosha. The amount of drop in strike–slip component and the corresponding increase of thrusting component may be induced by a local change in fault strike from the general N80°E to N70°E. Measurements of striations on the fault plane give the ratio between the strike–slip and reverse components of movements increasing from 1 near the village of Ardineh (Ar in Fig. 1) to 2 near Mosha.

Thus, the Ipak, Mosha, and, perhaps, North Tehran fault zones have the sinistral component of motion dominating over the reverse component, its average rate exceeding 1 mm/a for the Ipak and Mosha zones.

5. Discussion

In terms of active tectonics, the principal differences between the northwestern and the southeastern Zagros lie in orientations of major dextral faults and in their relationships with young thrusts and folds. In the northwestern Zagros, right lateral movements concentrate on the Main Recent Fault zone, while active thrusting and accompanying folding spread over the adjacent part of the Mesopotamian foredeep. In the southeastern Zagros, the major strike–slip faults stretch obliquely to the main trend of Zagros and, gradually curving, merge in their southeastern terminations with the NW – SE-trending thrusts and folds. In the Fars Province, the southwestern limit of the area subjected to active faulting and folding is about 100 km further southwest relative to its location in the northwestern Zagros. The linking structure between the two segments of the southwestern frontline of active deformations is the Borazjan zone.

One of the questions stemming from what was outlined above may thus relate to how the transition between the two segments of the single Zagros fault-and-fold belt occurs when described in terms of active faulting. Two end interpretations seem possible.

Firstly, oblique strike–slip faults of the southeastern Zagros look much like the faults splaying off the Main Recent Fault of Zagros and borrowing their strike–slip components of movements. If this is a case, the Main Recent Fault must be then interpreted as extending, in fact, farther southeast than its single-line segment does, dying out well inside the Fars Province and spreading its lateral motion there nearly over the whole Zagros width.

An alternative interpretation focuses on the fact that none of the oblique faults starts just from the line of the Main Recent Fault. The Kazerun fault, which is the largest of them, emanates in the north as the fault with no clear evidences of strike–slip movement and reveals many of such evidences only in its southern half. Then, all the oblique faults turn southeasterly into Zagros-parallel reverse and thrust faults that closely associate with folds, and thus come out to be just segments of single longer arched fault structures. If so, the oblique faults may have developed to accommodate some southwestward advancement of portions of sedimentary cover and probably of its basement and, consequently, broadening of Zagros within its Fars Province. This specificity of the Fars may relate, at least partially, to its higher mobility provided by both more mafic composition of its basement and a thick widespread evaporitic horizon (the Hormoz Formation) at the base of the sedimentary cover, compared with the neighboring northwestern part of Zagros.

In general, coeval existence of both transverse shortening and along-strike movements in the northwestern Zagros, spatially separated, suggests that interaction of the Arabian plate with the Iranian block proceeds mainly in an oblique collision mode.

Either of the two interpretations of the N–S-trending strike–slip faults of the southeastern Zagros implies that the latter is where along-belt tectonic movements cease. This implies that the southeastern Zagros may be where the oblique plate interaction gives place to essentially normal collision.

The Main Recent Fault of Zagros and its possible southern continuations are not the only strike–slip faults that have been accommodating the northern drift of the Arabian plate. There are several active faults to the northeast of Zagros that make a fault system between the Sanandaj–Sirjan zone, with probably Mesozoic age of the Earth's crust consolidation and Iranian microplate. These active fragments are the North Tebriz, Indes, Kashan–Zephreh, and Deh Shir faults (19 – 22 in Fig. 1), all of them combining dextral and reverse movements (Berberian, 1976; Hessami and Jamali, 1996). Together with the W-trending sinistral reverse fault system of the Tehran region, they probably reflect a rather rapid east-directed motion of the Iranian microplate, away from the north-moving Arabian plate.

References

Ambraseys, N.N., 1963. The Buyin–Zara (Iran) earthquake of 1 September 1962: a field report. Bull. Seismol. Soc. Am. 53, 705–740.

Bachmanov, D.M., 2001. Age zoning of coarse molasse in the outer zagros and migration of the recent orogeny. Geotektonika 35 (4), 505–509.

Berberian, M., 1976. Contribution on the Seismotectonics of Iran: Part I. Geological Survey of Iran, Tehran. 517 pp.

Berberian, M., 1981. Active faulting and tectonics of Iran. In: Cupta, H.K., Delany, F.M. (Eds.), Zagros–Hindukush–Himalayas Geodynamic Evolution. American Geophysical Union, Geodynamics Series 3, Washington, DC, pp. 33–69.

Berberian, M., 1994. Natural Hazards and the First Earthquake Catalogue of Iran: Vol. I. Historical Hazards in Iran Prior to 1900. IIEES, Tehran. 604 pp.

Berberian, M., Qorashi, M., Jackson, J.A., Priestly, K., Wallace, T., 1992. The Rudbar–Tarom earthquake of 20 June 1990 in NW Persia: preliminary field and seismological observations and its tectonic significance. Bull. Seismol. Soc. Am. 82, 1726–1755.

Hessami, Kh.T., Jamali, F.H., 1996. Active faulting in Iran. J. Earthq. Predict. Res. 5, 403–412.

Moinfar, A., Mahdavian, A., Maleki, E., 1994. Historical and instrumental earthquakes data collection of Iran. Mahab Ghodss Co., Tehran, 450 pp. of the recent orogeny. Geotectonics 35 (6), 505–509.

Saroglu, F., 1988. Age and offset of the North Anatolian fault. METU J. Pure Appl. Sci. 21 (1–3), 65–79.

Tchalenko, J.S., 1975. Seismotectonic framework of the North Tehran fault. Tectonophysics 29, 411–420.

Tchalenko, J.S., Ambraseys, N.N., 1970. Structural analysis of the Dashte–Bayas (Iran) earthquake fractures. Bull. Geol. Soc. Am. 81, 41–60.

Tchalenko, J.S., Braud, J., 1974. Seismicity and structure of the Zagros (Iran): the Main Recent Fault between 33° and 35°N. Philos. Trans. R. Soc. Lond. 277, 1–25.

Tchalenko, J.S., Berberian, M., 1975. Dasht-e–Bayaz fault, Iran: earthquake and earlier related structures in bed rock. Bull. Geol. Soc. Am. 86, 703–709.

Tchalenko, J.S., Braud, J., Berberian, M., 1974. Discovery of three earthquake faults in Iran. Nature 248, 661–663.

Tectonic Map of Southcentral Iran, 1973. Scale 1:2,500,000. National Irānian Oil Company—EPG. The Tehran Naqshé Printing House (in cooperation with T. Sādjedi).

Tectonic Map of Southwest Irān, 1976. Scale 1:2,500,000. National Irānian Oil Company—EPG. NCC. Offset Press, Teherān.

Wallace, R.E., 1977. Profiles and ages of young scarps, north-central Nevada. Bull. Geol. Soc. Am. 88, 1267–1281.

Wells, D.L., Coppersmith, K.J., 1994. New empirical relationships among magnitude, rupture length, rupture width, rupture area, and surface displacement. Bull. Seismol. Soc. Am. 84, 974–1002.